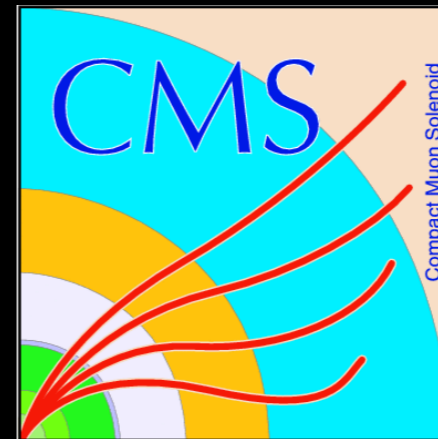


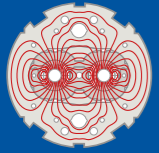
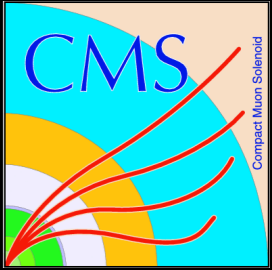
The High Granularity Calorimeter upgrade for of the CMS detector for the High Luminosity LHC



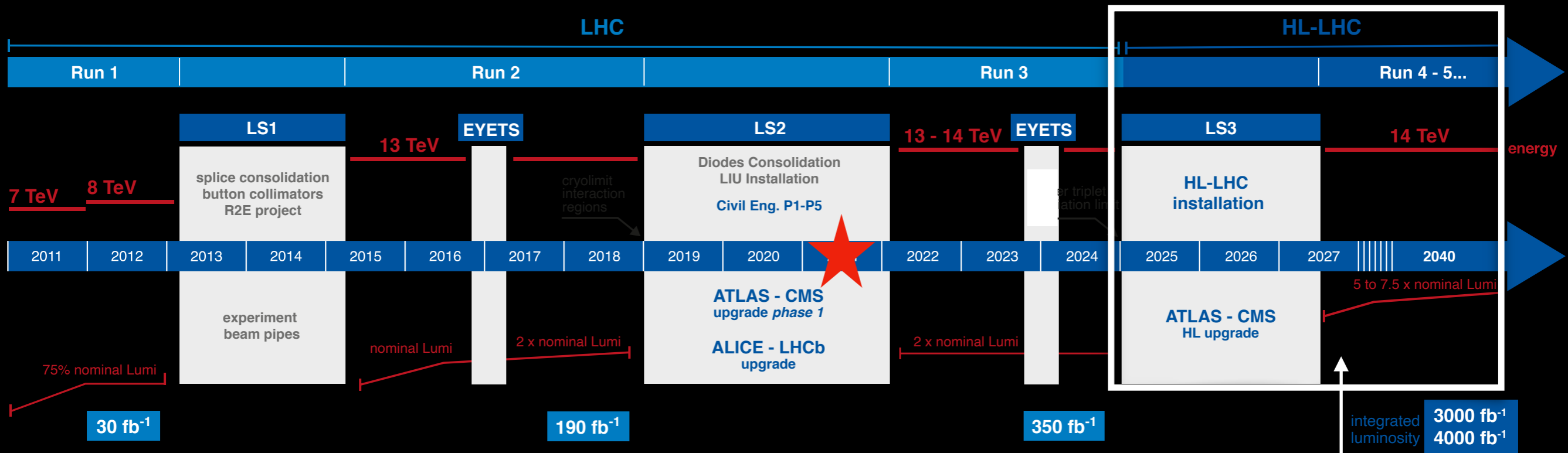
Saptaparna Bhattacharya, on behalf of the CMS Collaboration
2021 Meeting of the Division of Particles and Fields of the American Physical Society



The upgrade schedule



LHC / HL-LHC Plan



HL-LHC TECHNICAL EQUIPMENT:



HL-LHC CIVIL ENGINEERING:

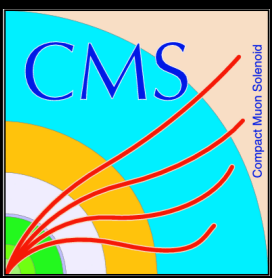


Radiation damage foreseen that will necessitate the replacement of the endcap detectors
CMS-TDR-019

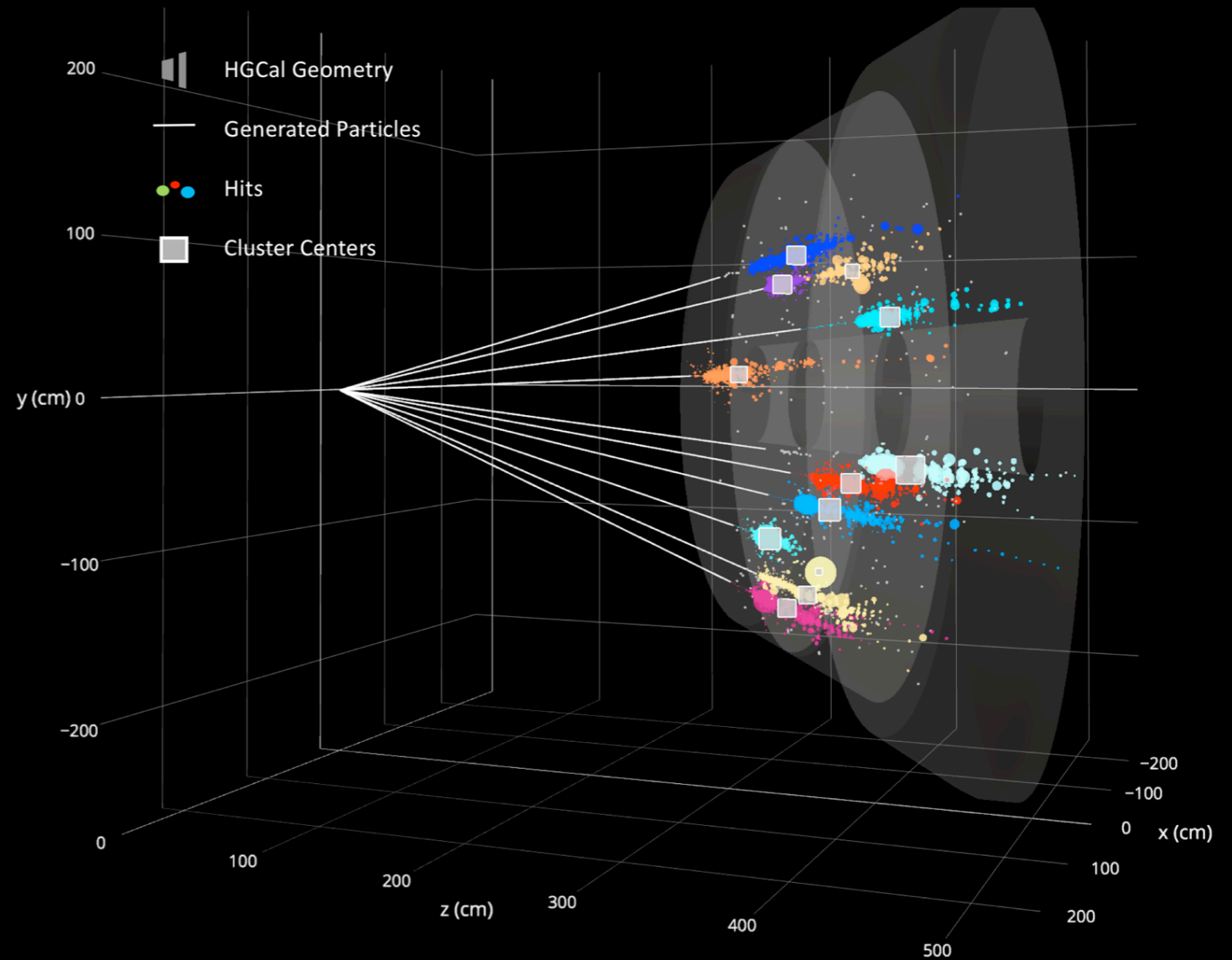
★ We are here



Unprecedented granularity



- The High Granularity Calorimeter (HGCal) will possess unprecedented spatial granularity
- 3D visualization of showers
- Excellent energy resolution in the endcaps
- Enables identification of electrons, photons, pions and even muons
- Timing capabilities allow the ability to distinguish close-by showers



Visualization of showers from 10 generated pions

<https://crd.northwestern.edu/visualizations/visualization-of-reconstruction-of-CMS-HGCal/>

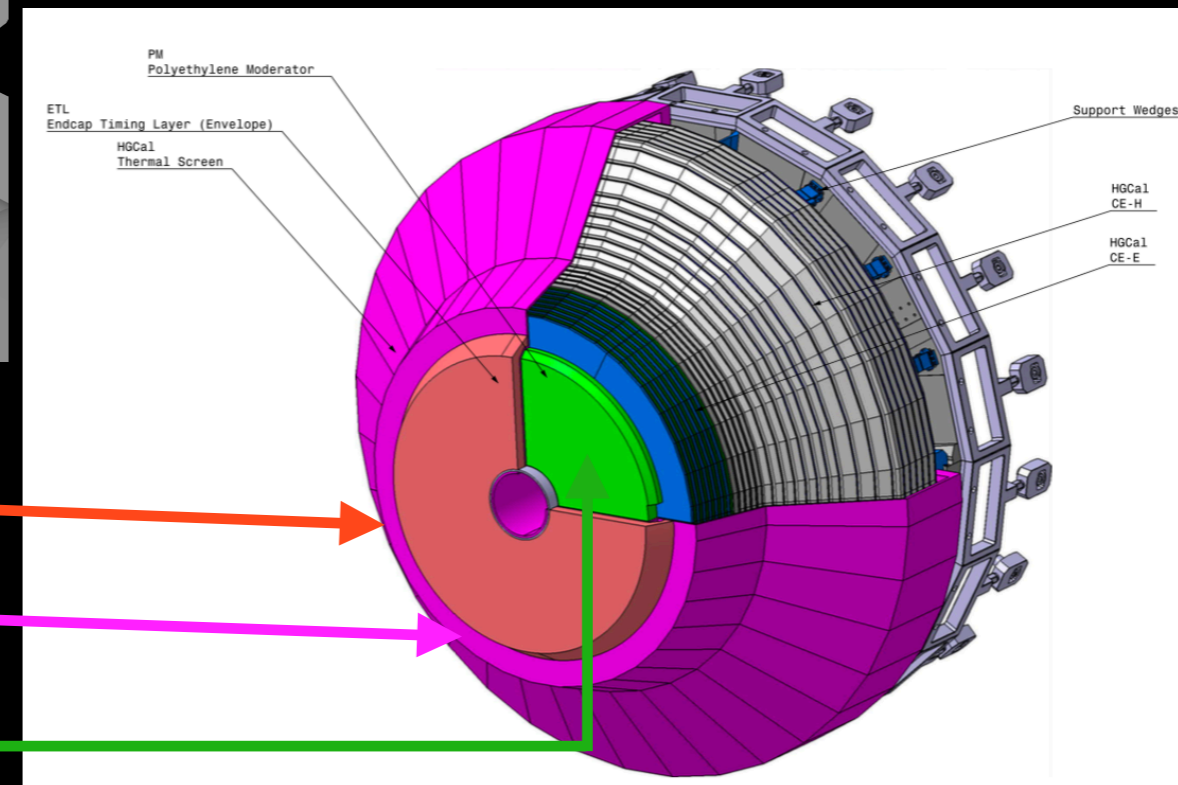
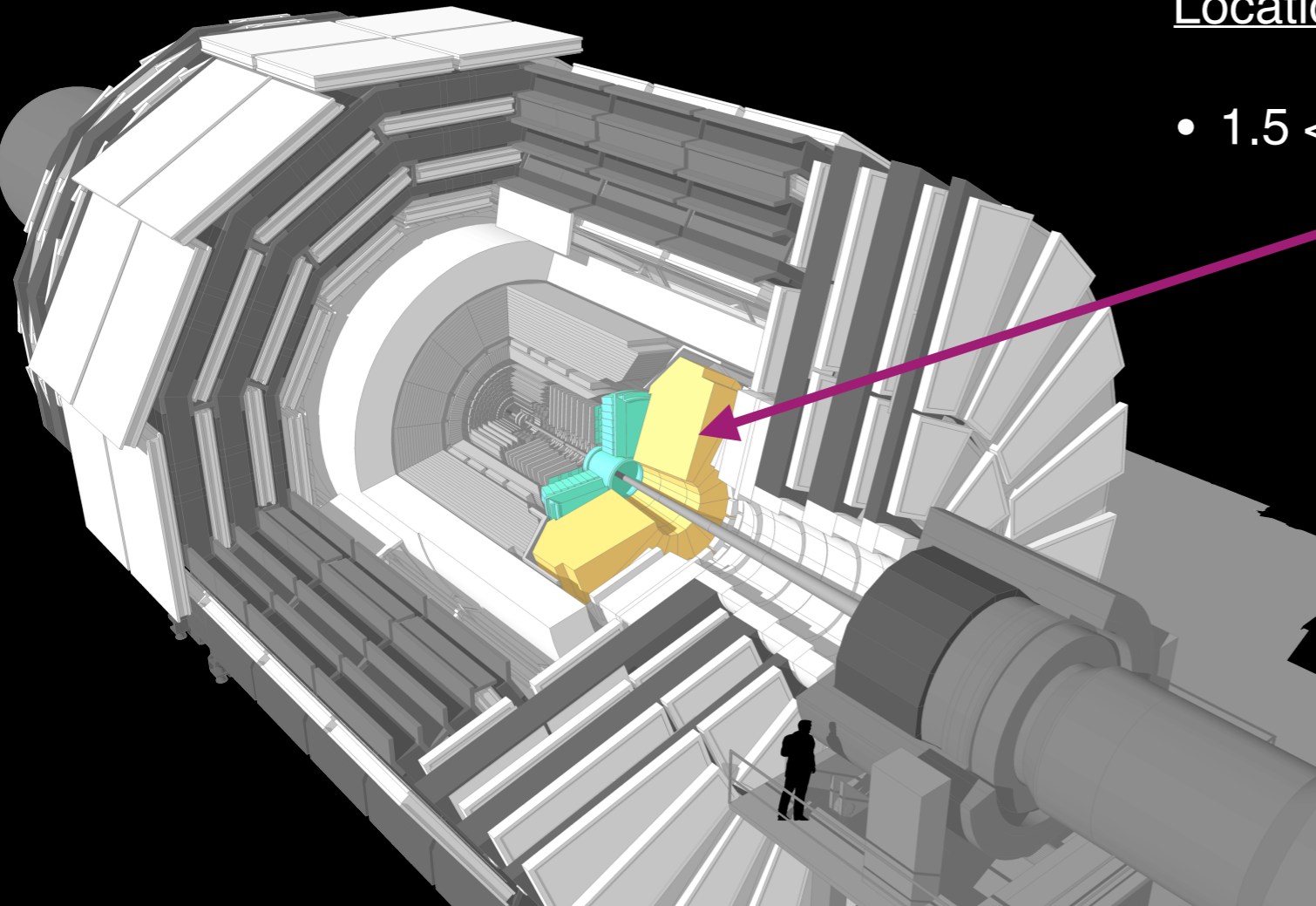
The location of the HGCal

Location of the HGCal:

- $1.5 < \eta < 3.0$

• Related R&D:

- DAQ system designed to cope with the large amount of space-energy-time information in the HL-LHC conditions
- Considerable R&D for software and computing needs and development of efficient algorithms for reconstruction



- Endcap Timing Layer
- HGCal Thermal Screen
- Polyethelene Moderator

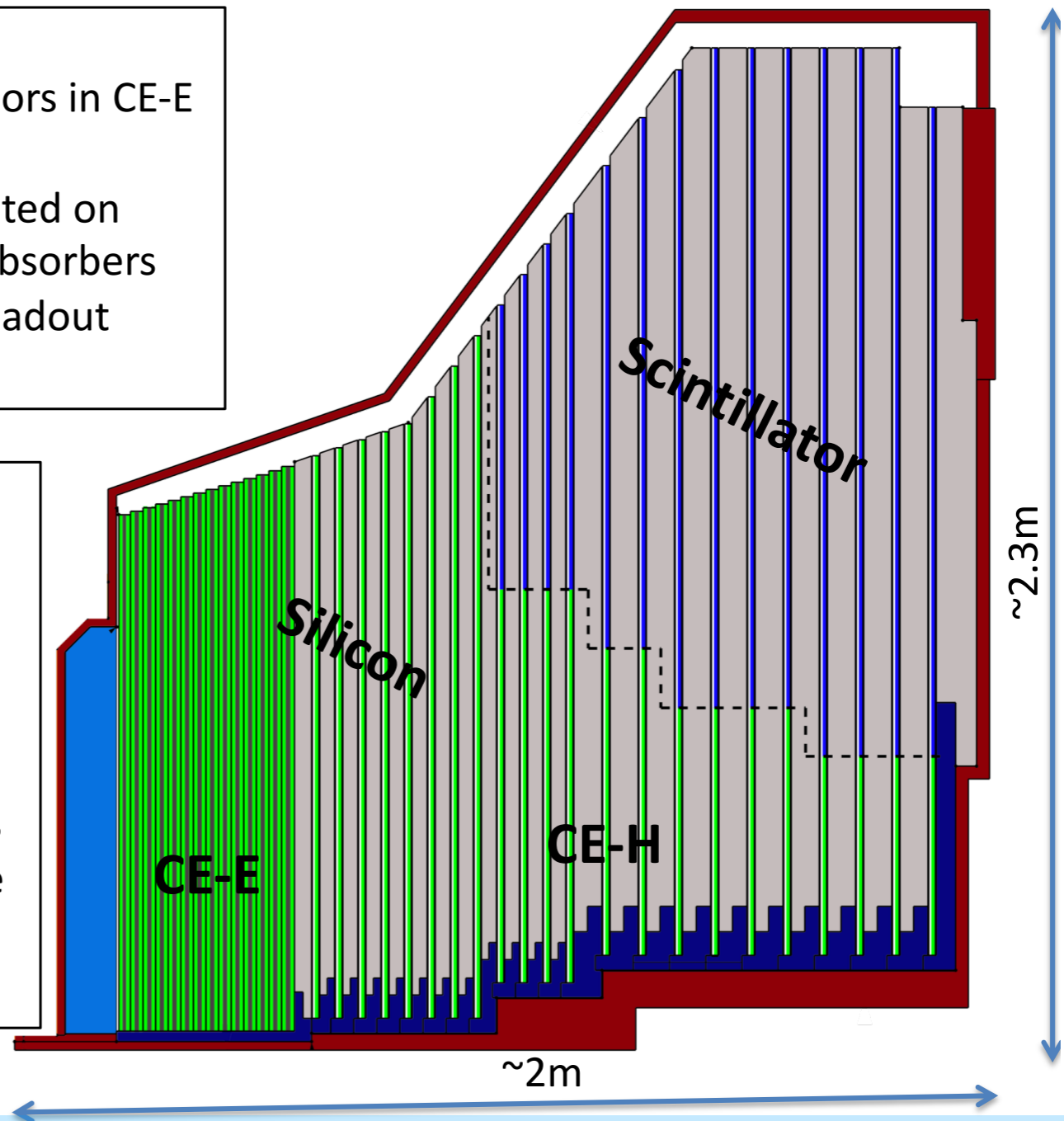
The design of the HGCAL

Active Elements:

- Hexagonal modules based on Si sensors in CE-E and high-radiation regions of CE-H
- “Cassettes”: multiple modules mounted on cooling plates with electronics and absorbers
- Scintillating tiles with on-tile SiPM readout in low-radiation regions of CE-H

Key Parameters:

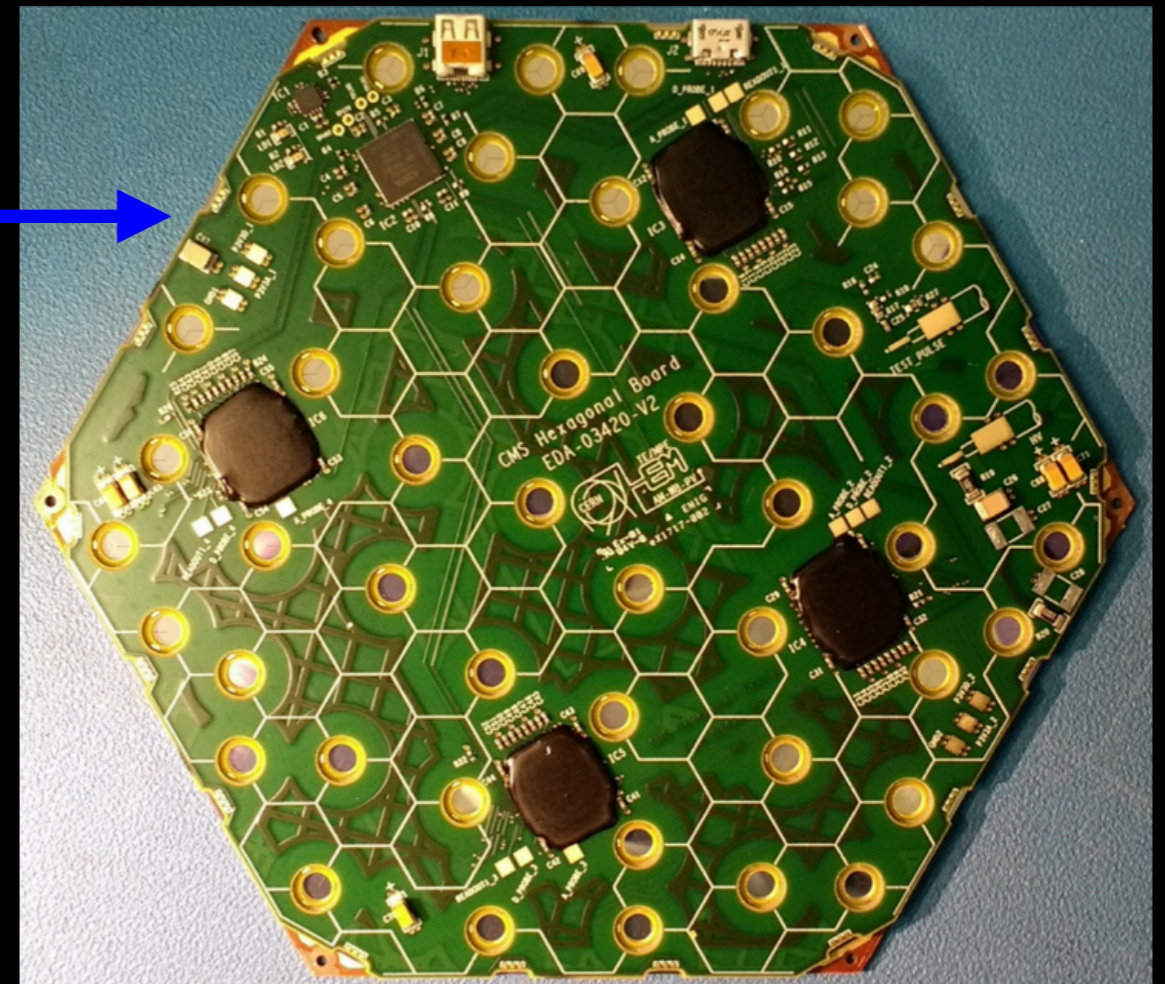
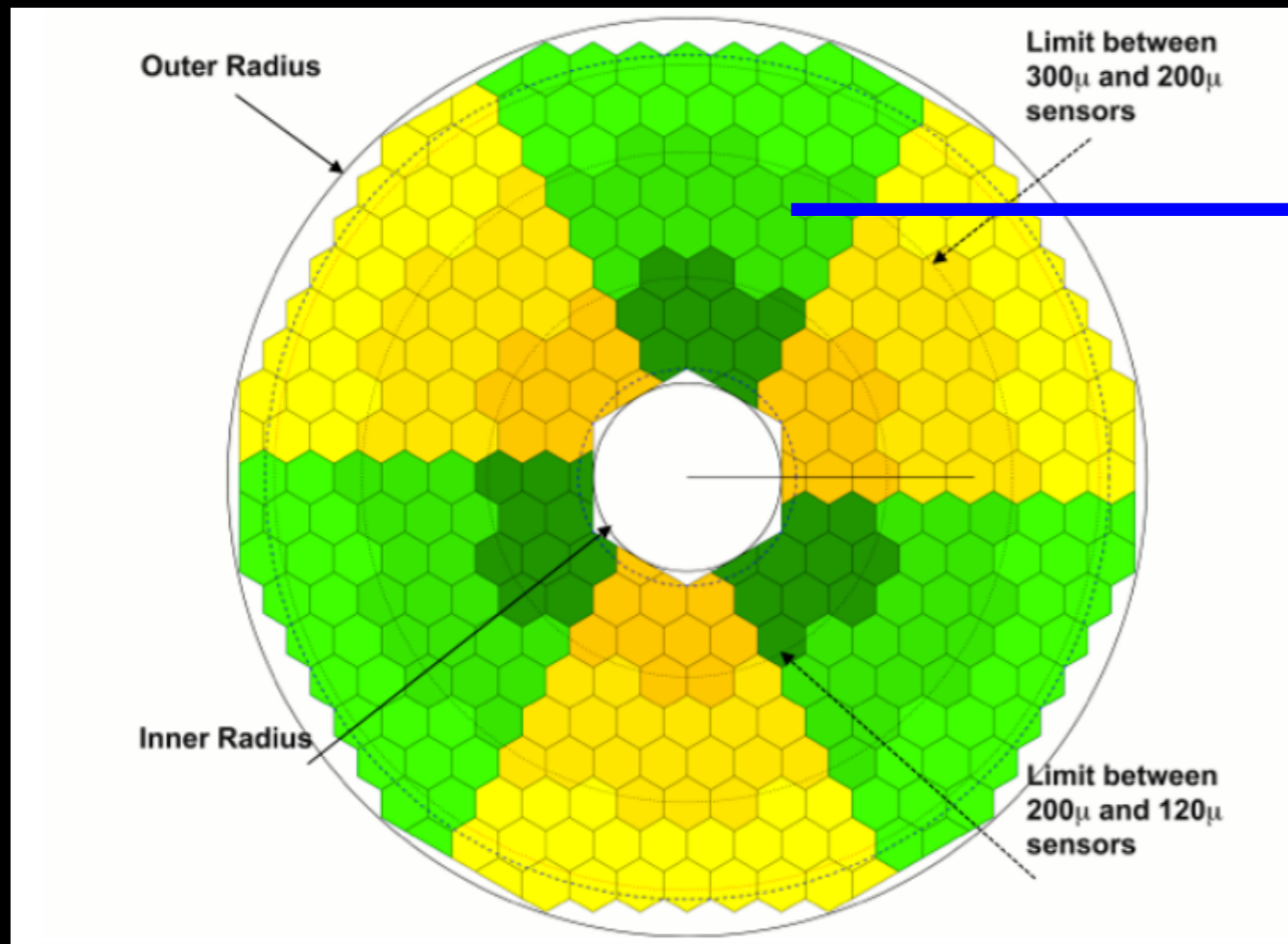
Coverage: $1.5 < |\eta| < 3.0$
 ~215 tonnes per endcap
 Full system maintained at -35°C
 ~620m² Si sensors in ~30000 modules
 ~6M Si channels, 0.5 or 1cm² cell size
 ~400m² of scintillators in ~4000 boards
 ~240k scint. channels, 4-30cm² cell size
 Power at end of HL-LHC:
 ~125 kW per endcap



Electromagnetic calorimeter (CE-E): **Si**, Cu & CuW & Pb absorbers, 28 layers, $25 X_0$ & $\sim 1.3\lambda$
 Hadronic calorimeter (CE-H): **Si** & **scintillator**, steel absorbers, 22 layers, $\sim 8.5\lambda$

Sensor layout in the silicon section

- HGCAL sensors will have 3 different active thicknesses:
 - optimized taking charge collection and operation conditions into account
 - 120 μm , 200 μm and 300 μm

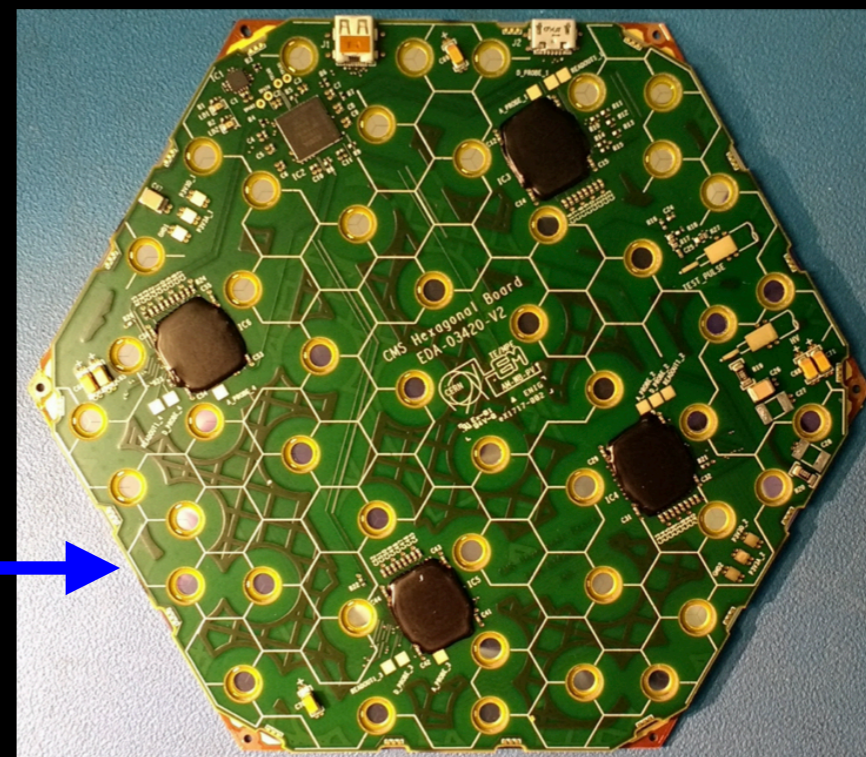
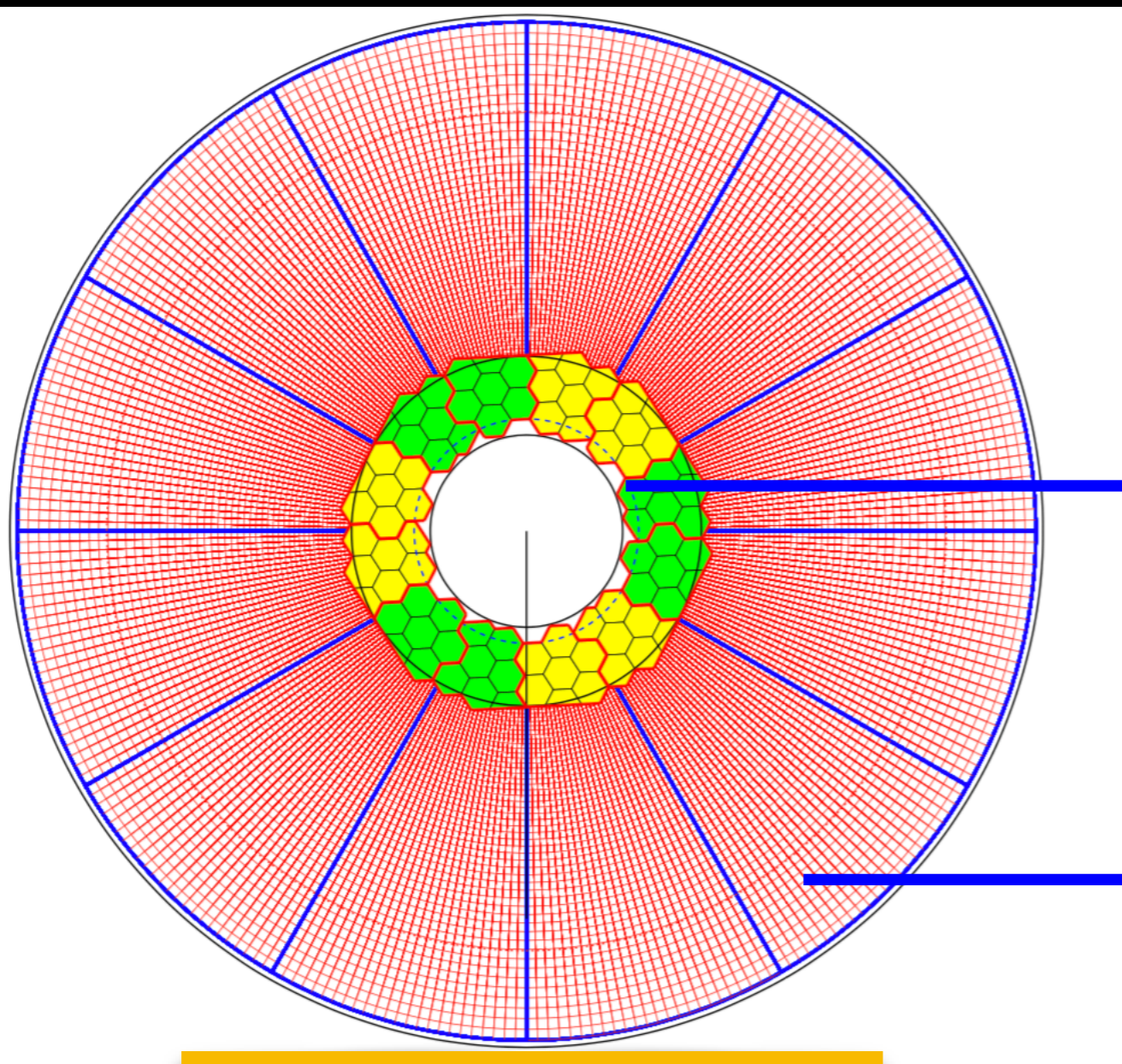


Dedicated talk on silicon sensors for the CMS HGCAL upgrade in this session

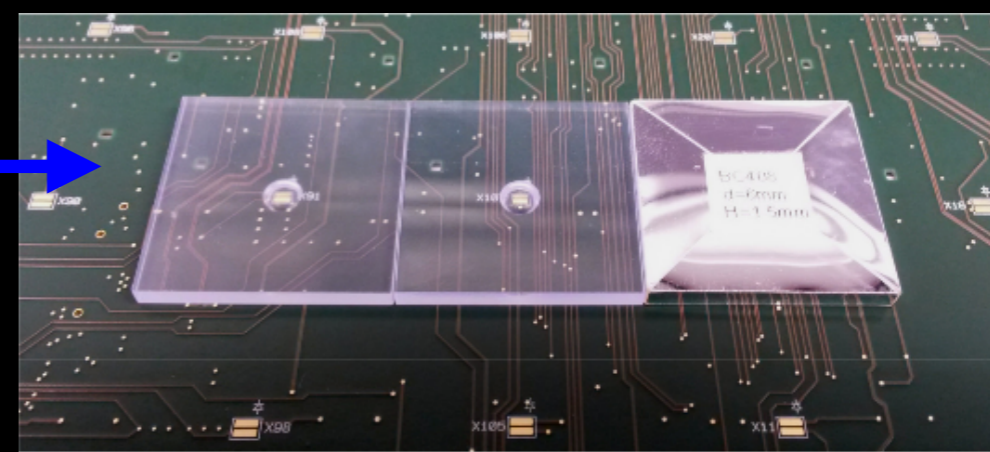
6 inch prototype module

Sensor layout in the scintillator section

- Hadronic section features silicon sensors and SiPM-on-tile readout sensors



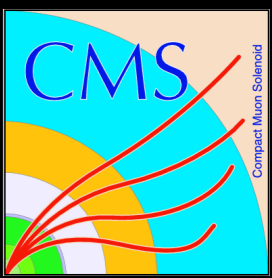
6 inch prototype module



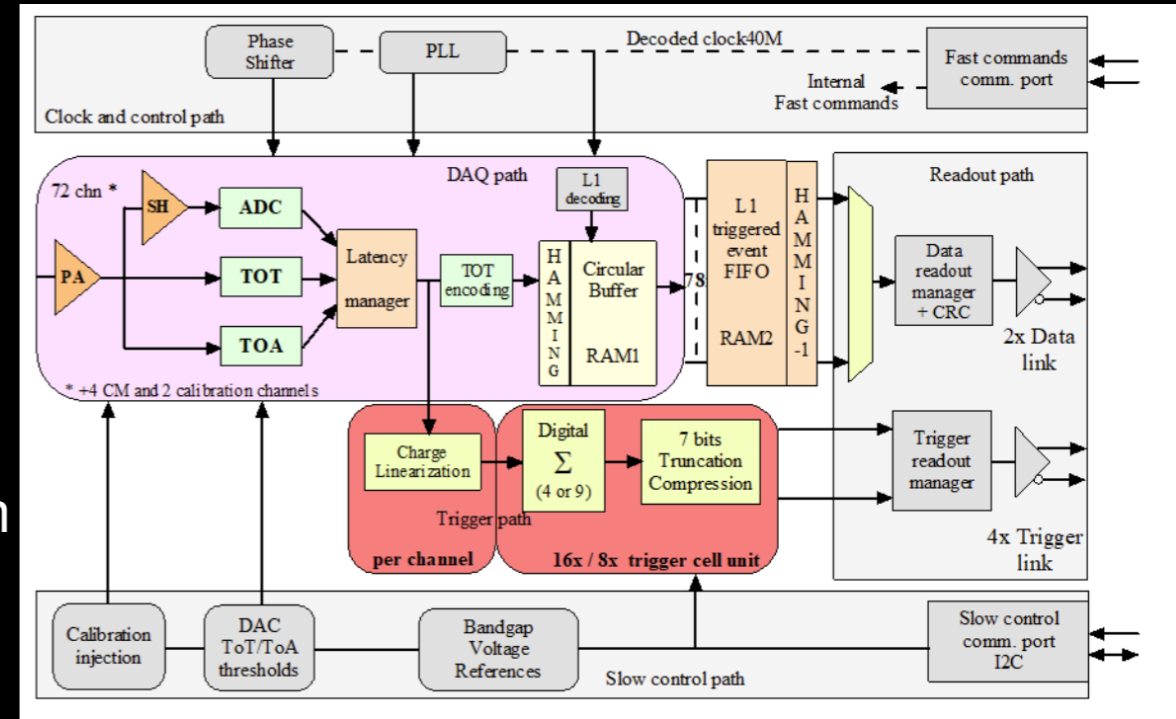
Dedicated talk on the SiPM-on-tile system of the CMS HGCal upgrade in this session



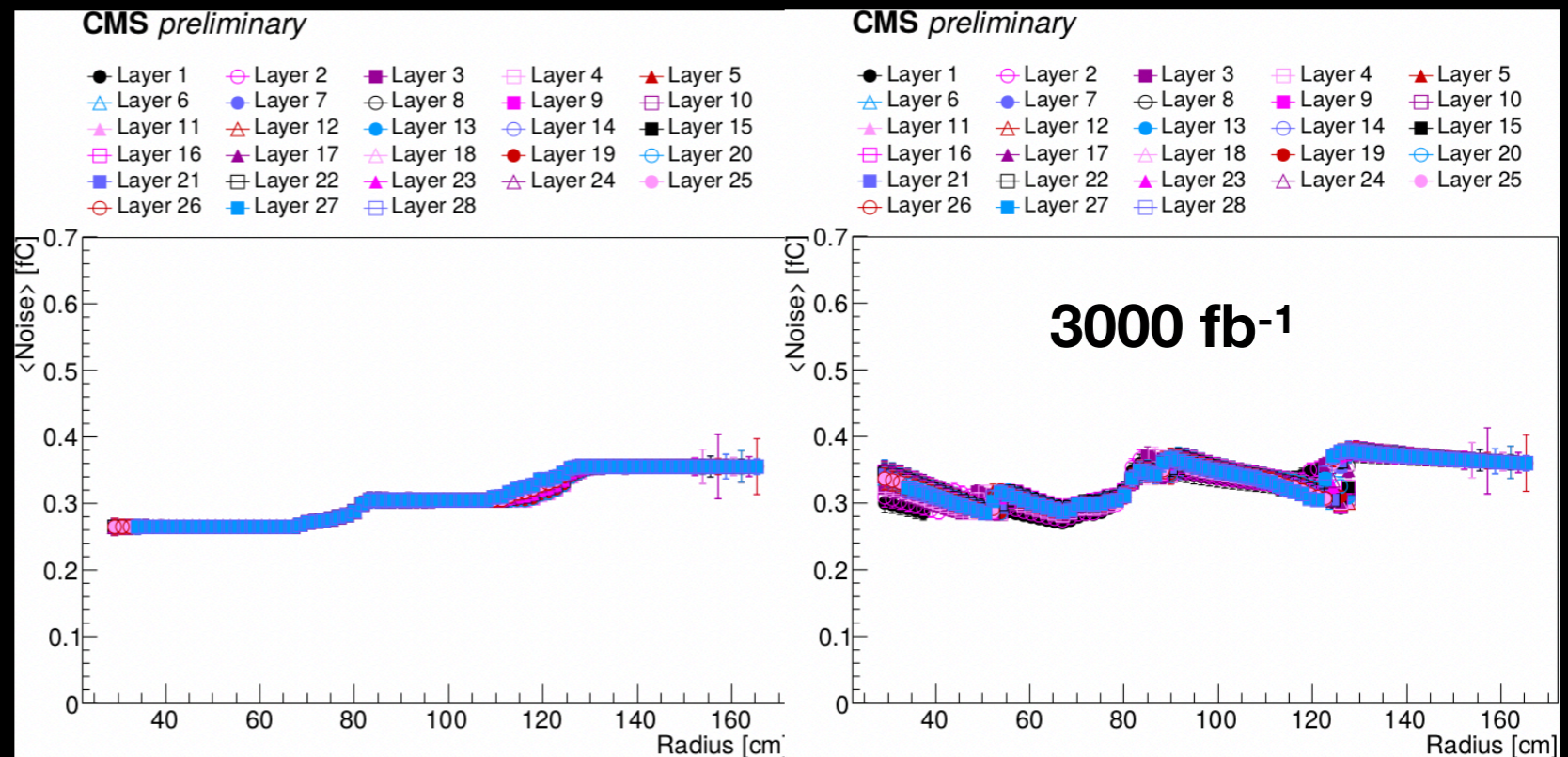
The HGCal Readout Infrastructure



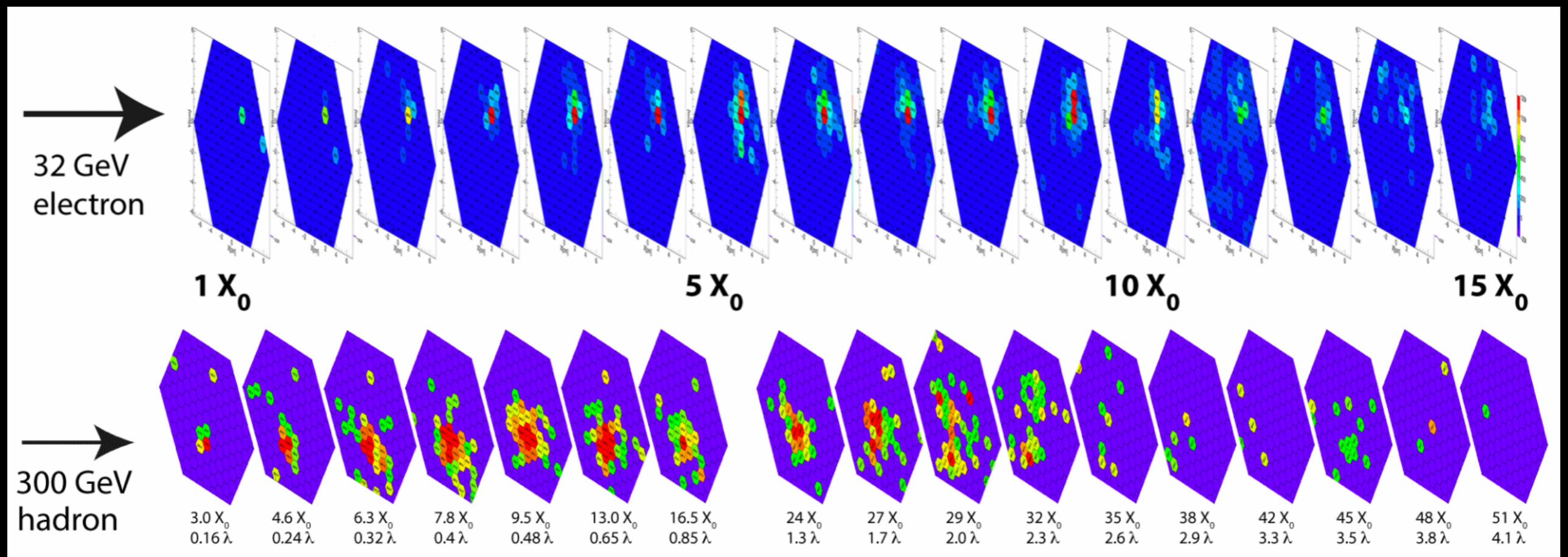
- HGCROC ASIC → signal amplification and shaping, digitization, triggering
- Concentrator ASIC (ECON) → aggregates data from a collection of HGCROCs
 - ECON performs trigger primitive data-processing with more than one possible algorithm
 - ECON performs zero suppression of triggered data



- The HGCROC increasingly realistic in the simulations with regard to inclusion of noise
- Performance stable across detector volume
- End-of-life conditions show some deterioration within tolerance

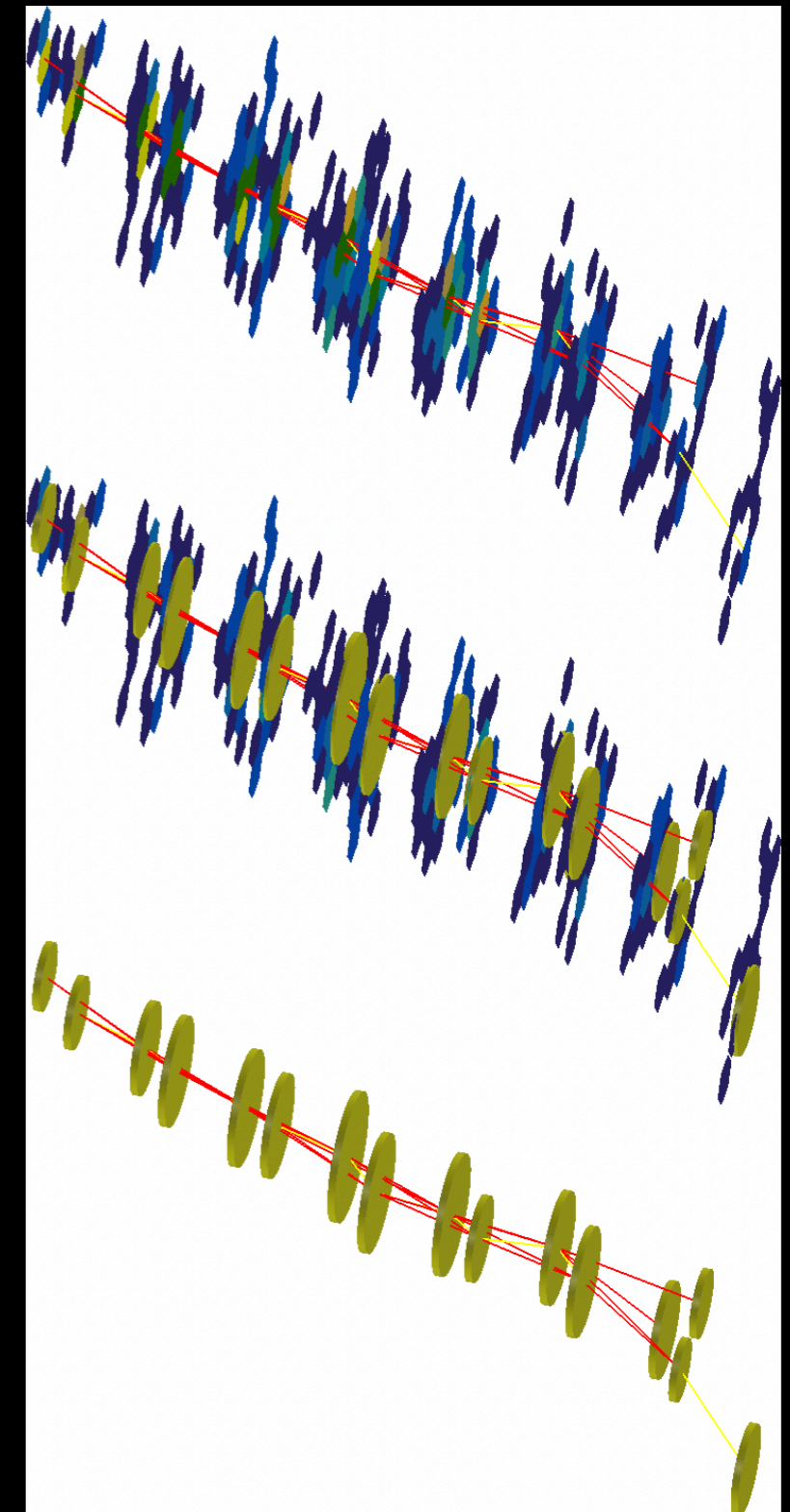
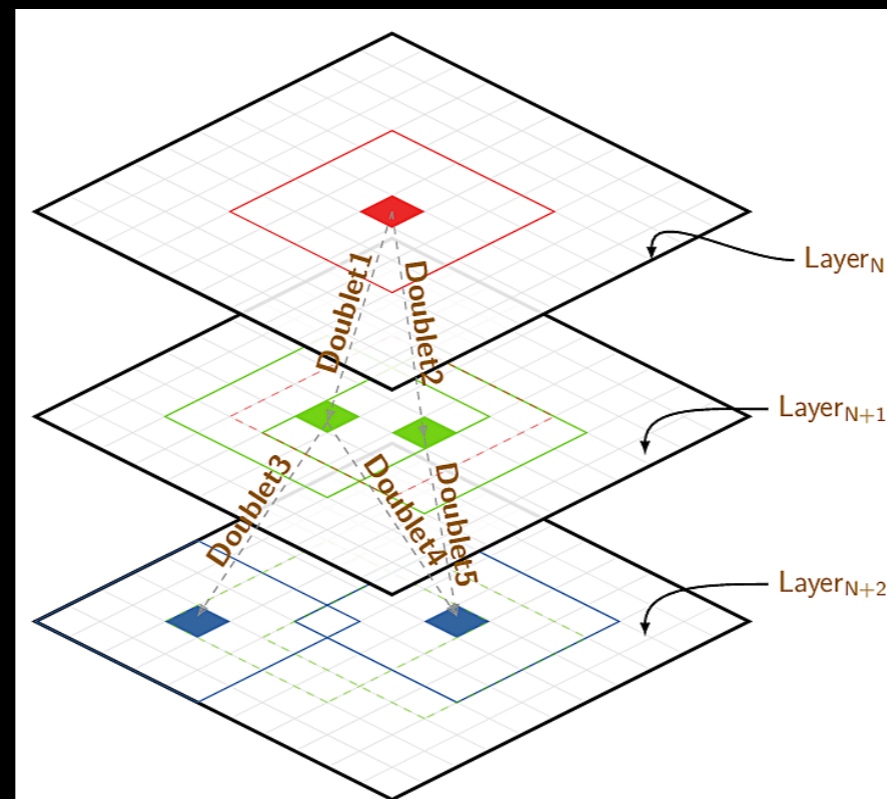


- Shower reconstruction in the HGCal is iteratively done in 2+1 dimensions
- Event displays from test beam data illustrate the proof of principle
- The 2D clusters are called “layer clusters” and are merged to form a single cluster → representative of the shower
- Amenable to an order of magnitude speed-up with GPUs

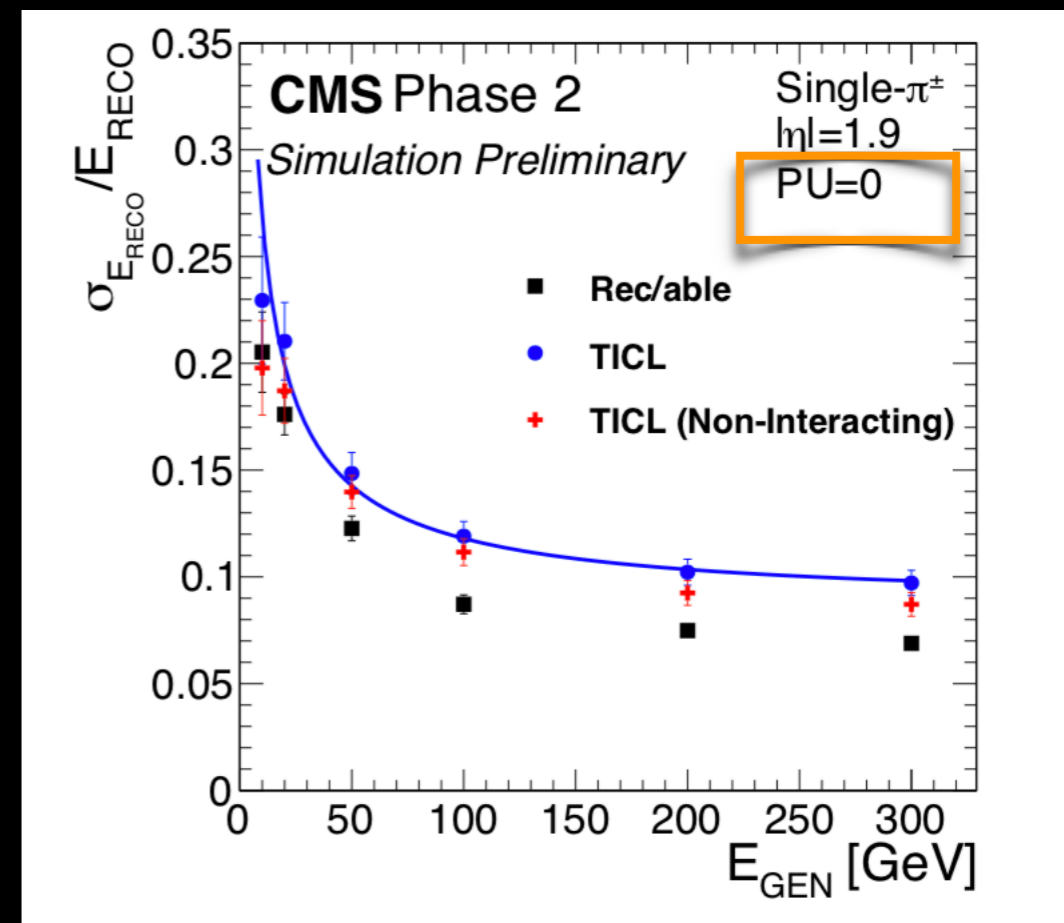
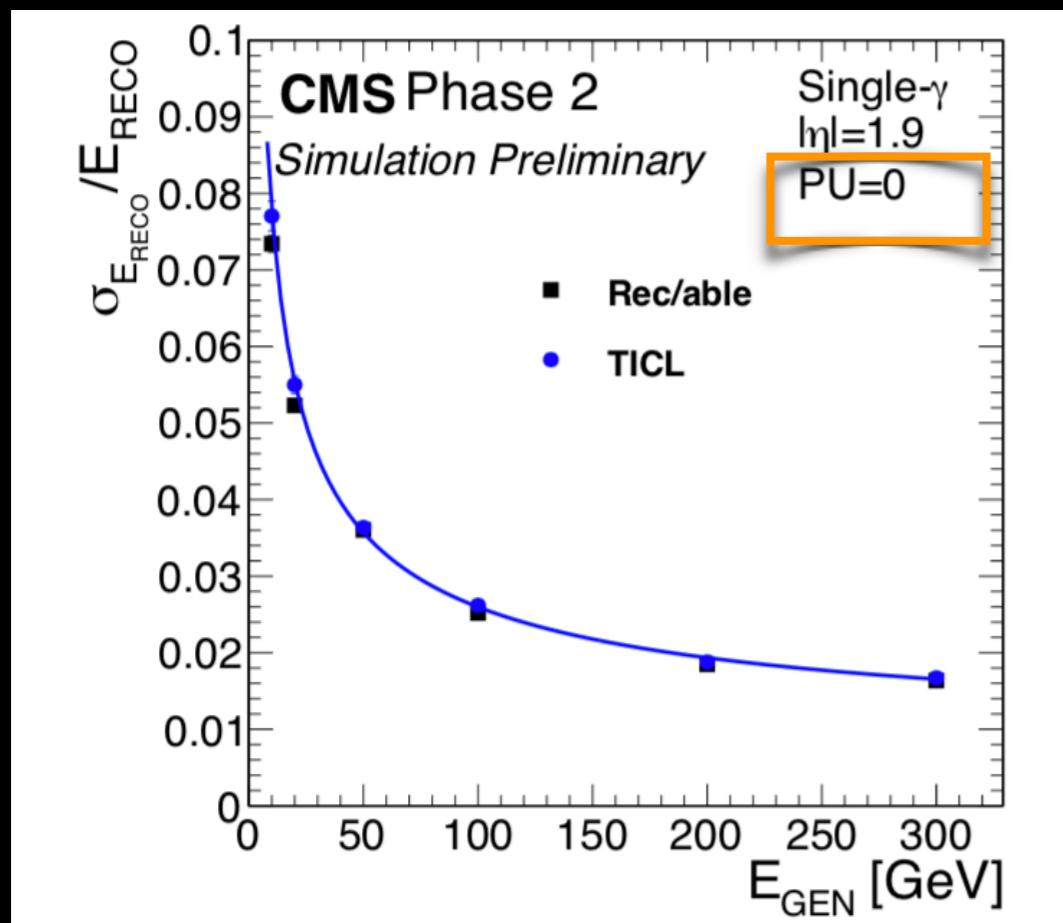


RecHits in the cells of each consecutive sensor

- Linking of 2D layer clusters to form 3D shower performed with a cellular automaton based pattern recognition algorithm
 - Involves window search from layer $N \rightarrow$ layer $N+1$ (creating a doublet) including compatibility criteria based on energy, timing, geometric constraints
- Simplified combinatorics if electromagnetic components removed before clustering hadronic block



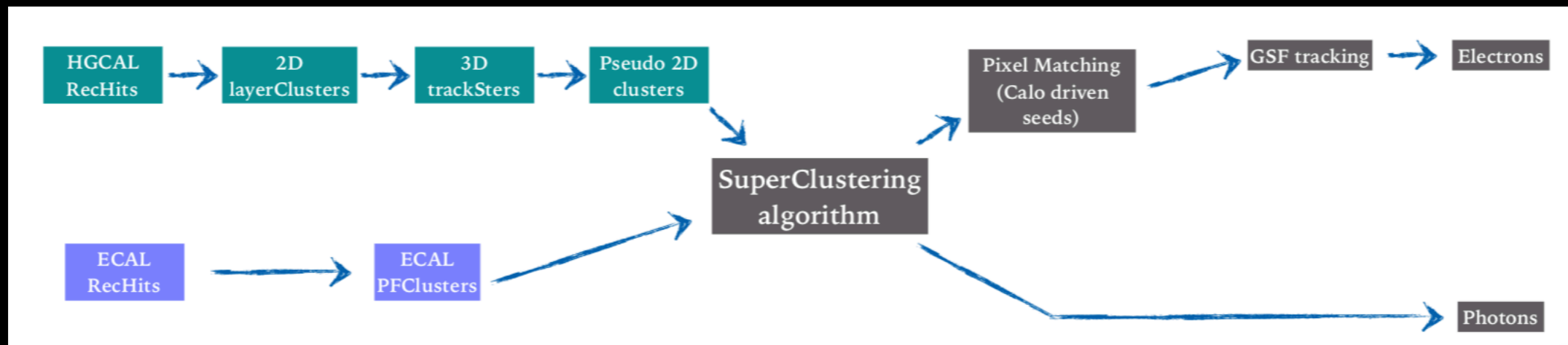
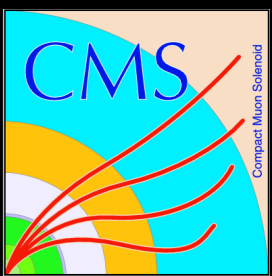
- The performance of the TICL algorithm in shower energy reconstruction is encouraging for both electromagnetic and hadronic showers
 - current approach collects all diffused components of the hadronic shower as a single object



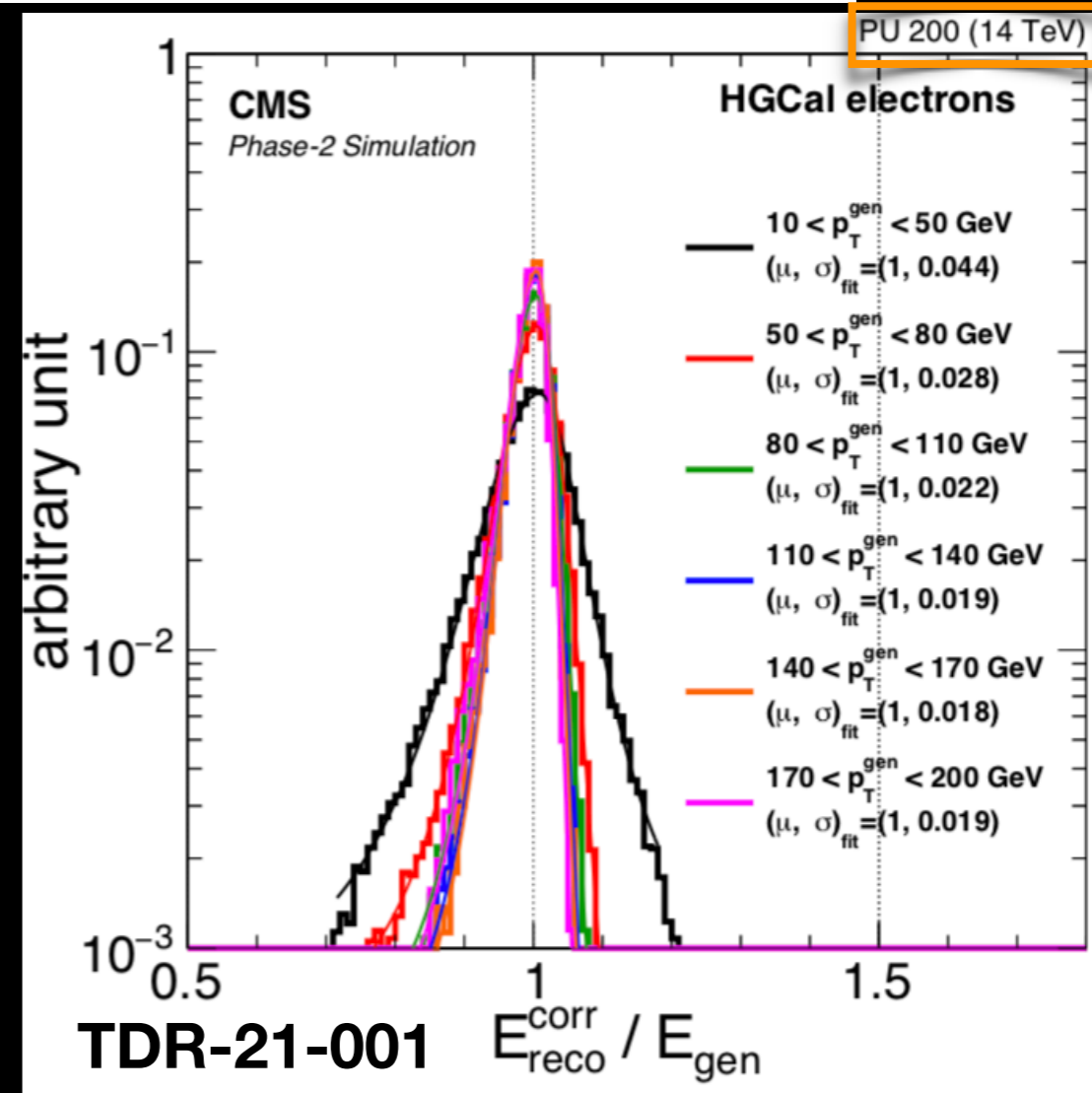
- **Rec/able:** The energy that can be reconstructed by summing the energy of all reconstructed hits pertaining to a generated particle
- **Non-interacting:** no interaction in the tracker volume



High Level Triggering (HLT) with TICL

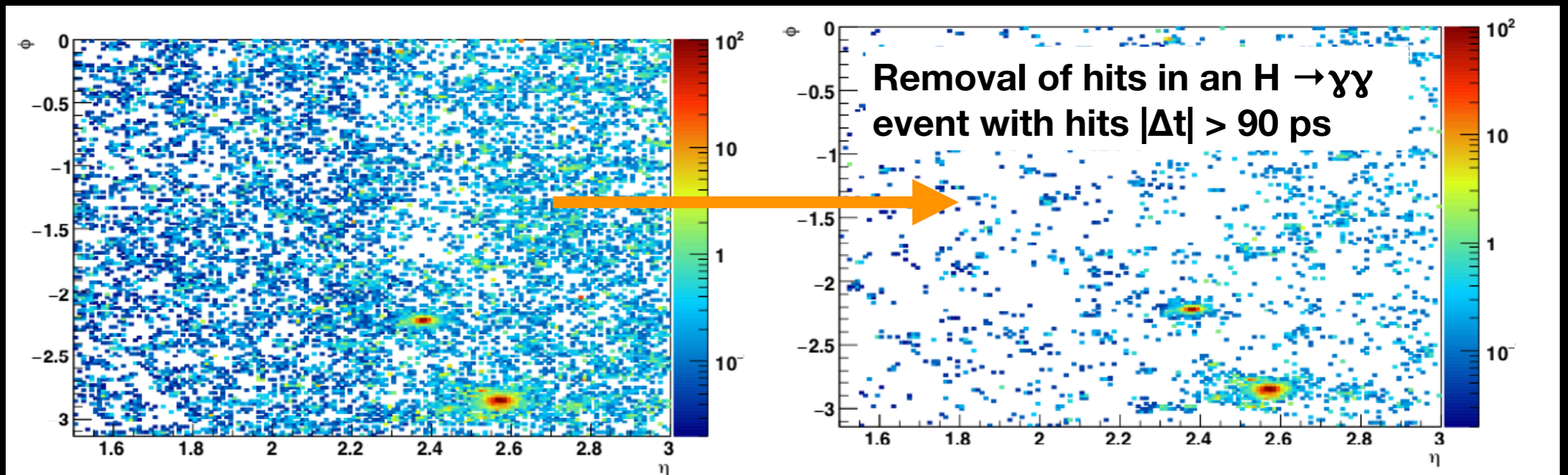
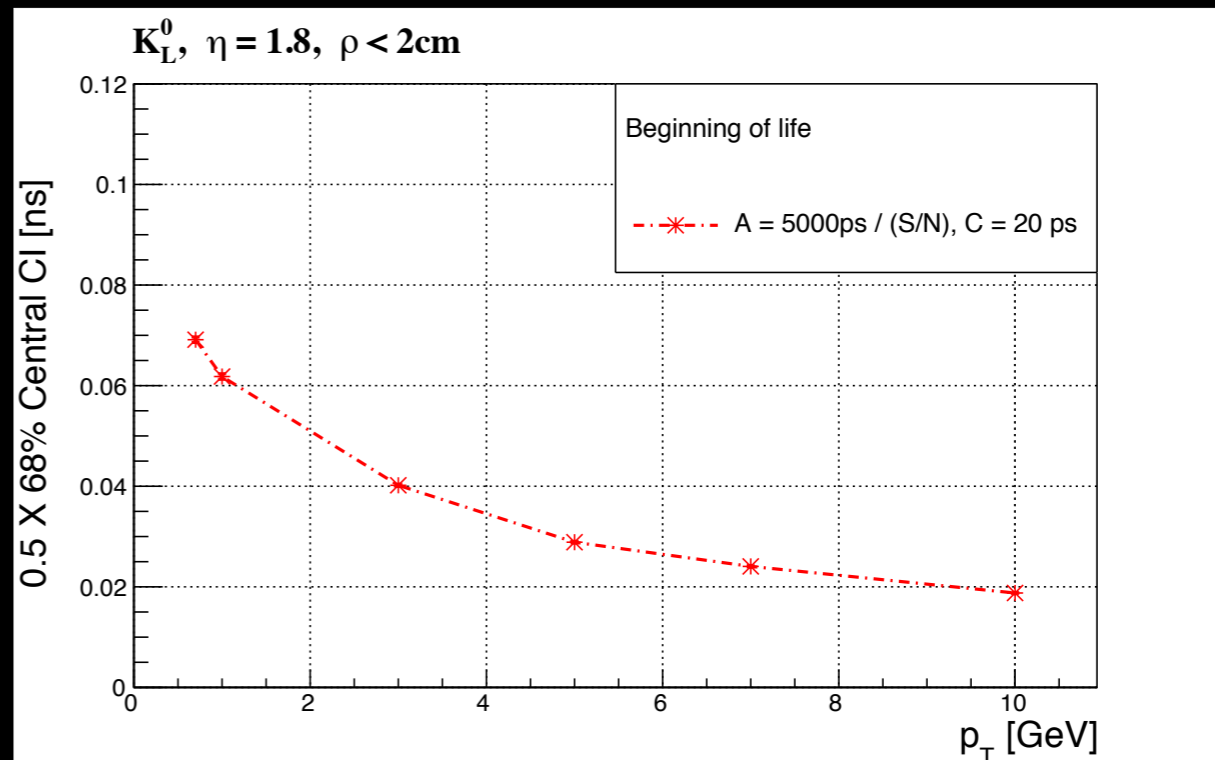


- HGAL reconstruction chain successfully implemented in trigger paths
- TICL algorithm optimized for HLT timing
- Multivariate regression (in use in Phase-I) used to further improve performance
 - inputs based on shower shape variables and ratios of hadronic and electromagnetic energy
- 2D layer clusters can be used to define calorimetric isolation specified at the HLT



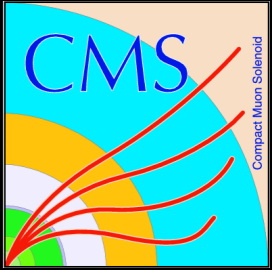
Timing Performance of the HGCAL

- Intrinsic silicon signal time resolution (\sim few ps) can be used to distinguish between close by showers
- Use $O(10$ ps) timing to individuate pileup particle showers

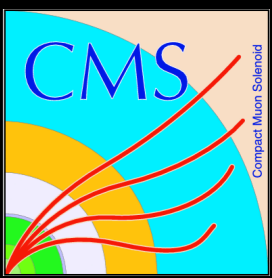




Conclusion



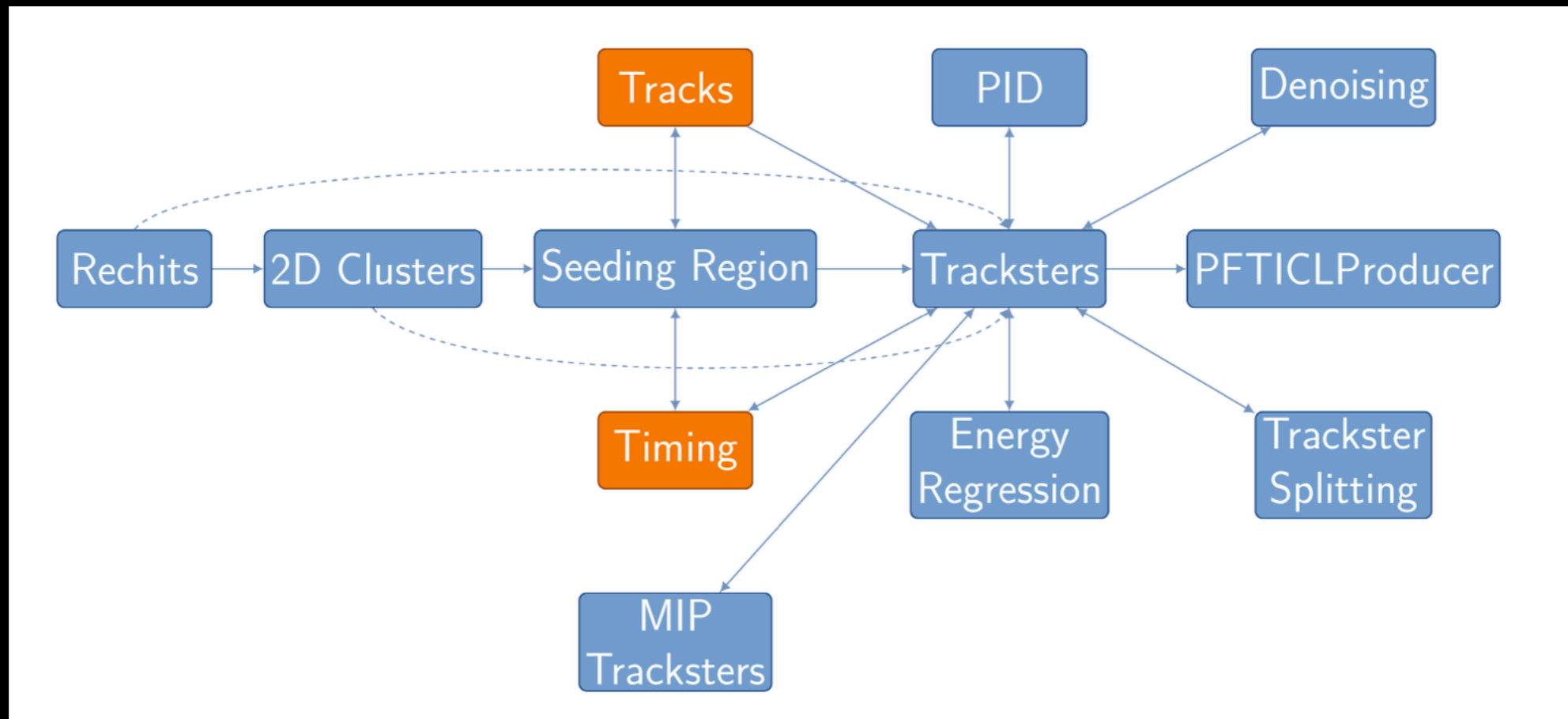
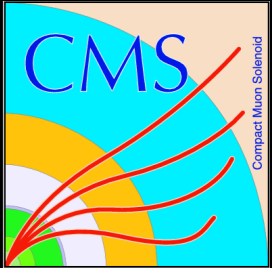
- A brief overview of the High-Granularity Calorimeter was presented
- The HGCAL provides unprecedented spatial granularity
- It enables excellent identification of electrons, photons, pions and even muons!
- It will be the first calorimeter at a collider with $O(10 \text{ ps})$ precision timing capabilities, leading to the identification and eventual mitigation of pile-up, one of the biggest challenges of the HL-LHC environment
- Sophisticated shower reconstruction algorithms needed and first steps in place



Additional Material



The TICL algorithm



The various steps of the TICL algorithm

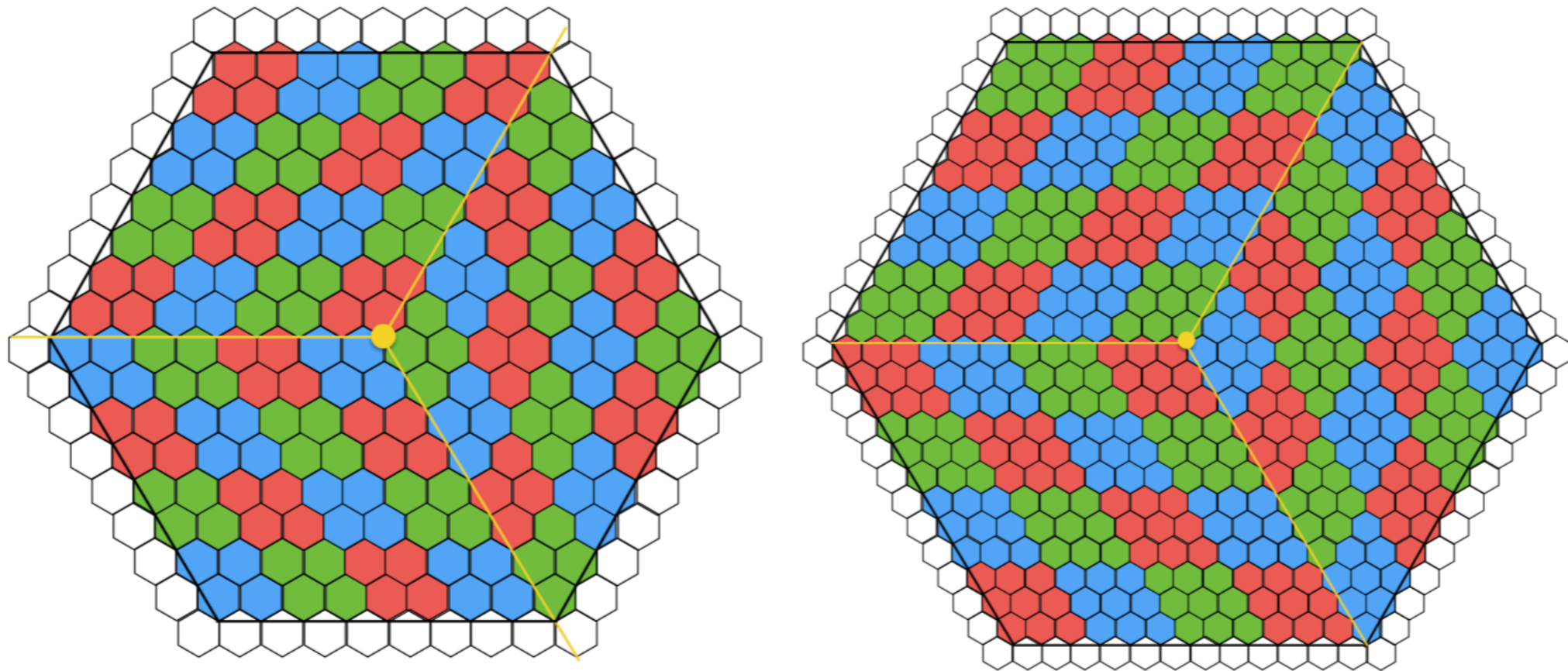
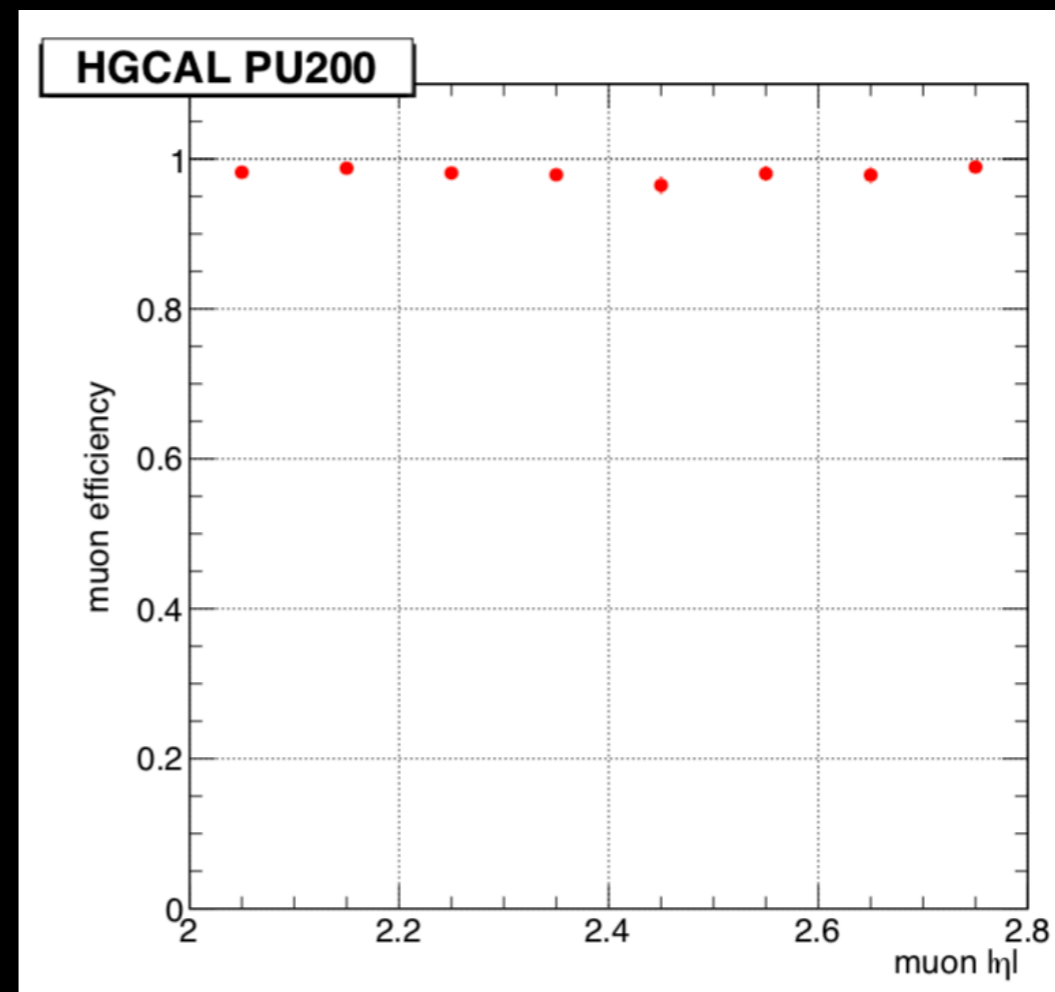
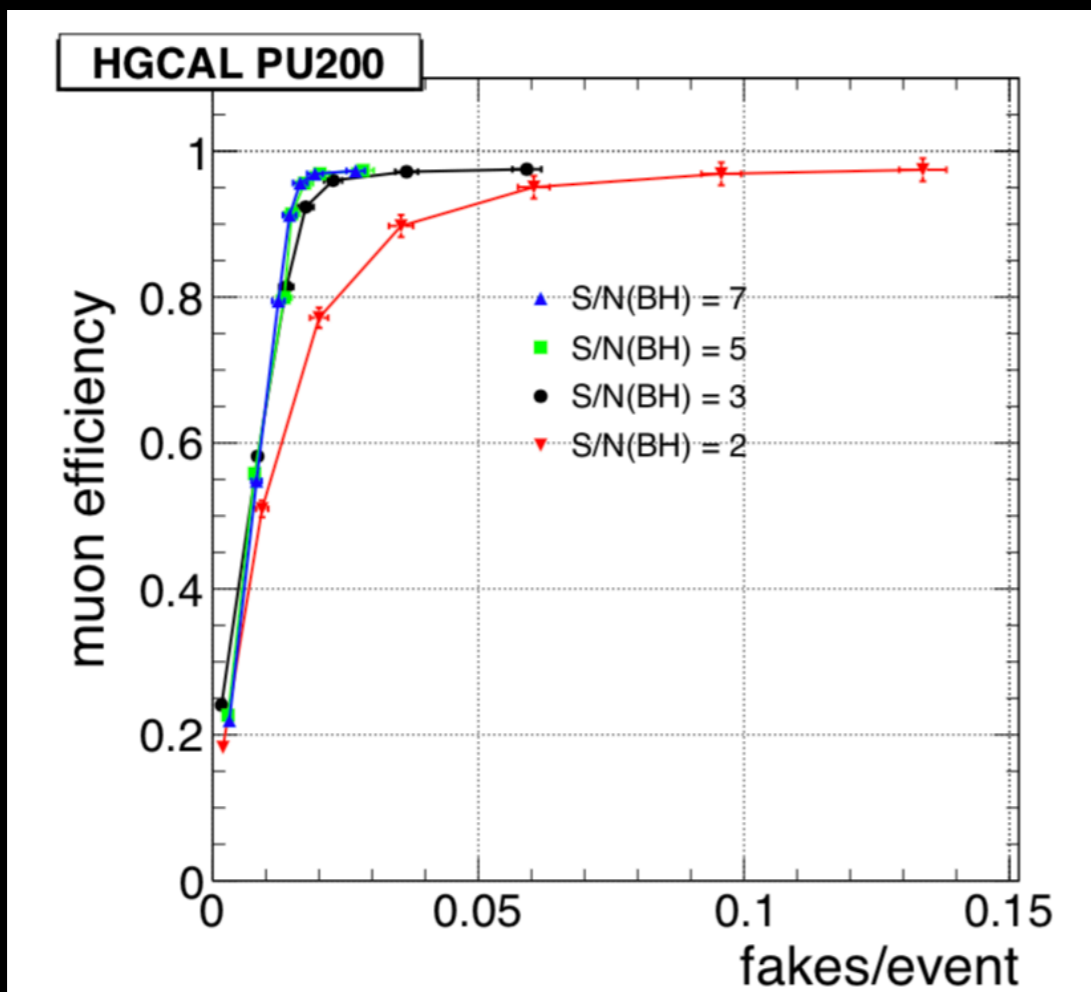


Figure 2.3: Schematic illustration of the three-fold diamond configuration of sensor cells on hexagonal 8'' silicon wafers, showing the groupings of sensor cells that get summed to form trigger cells, for the large, 1.18 cm^2 , sensor cells (left), and for the small, 0.52 cm^2 , cells (right).

<https://cds.cern.ch/record/2293646/files/CMS-TDR-019.pdf>

- Muon identification capabilities provided by the HGCAL for $2.0 < |\eta| < 2.8$ (in addition to ME0)

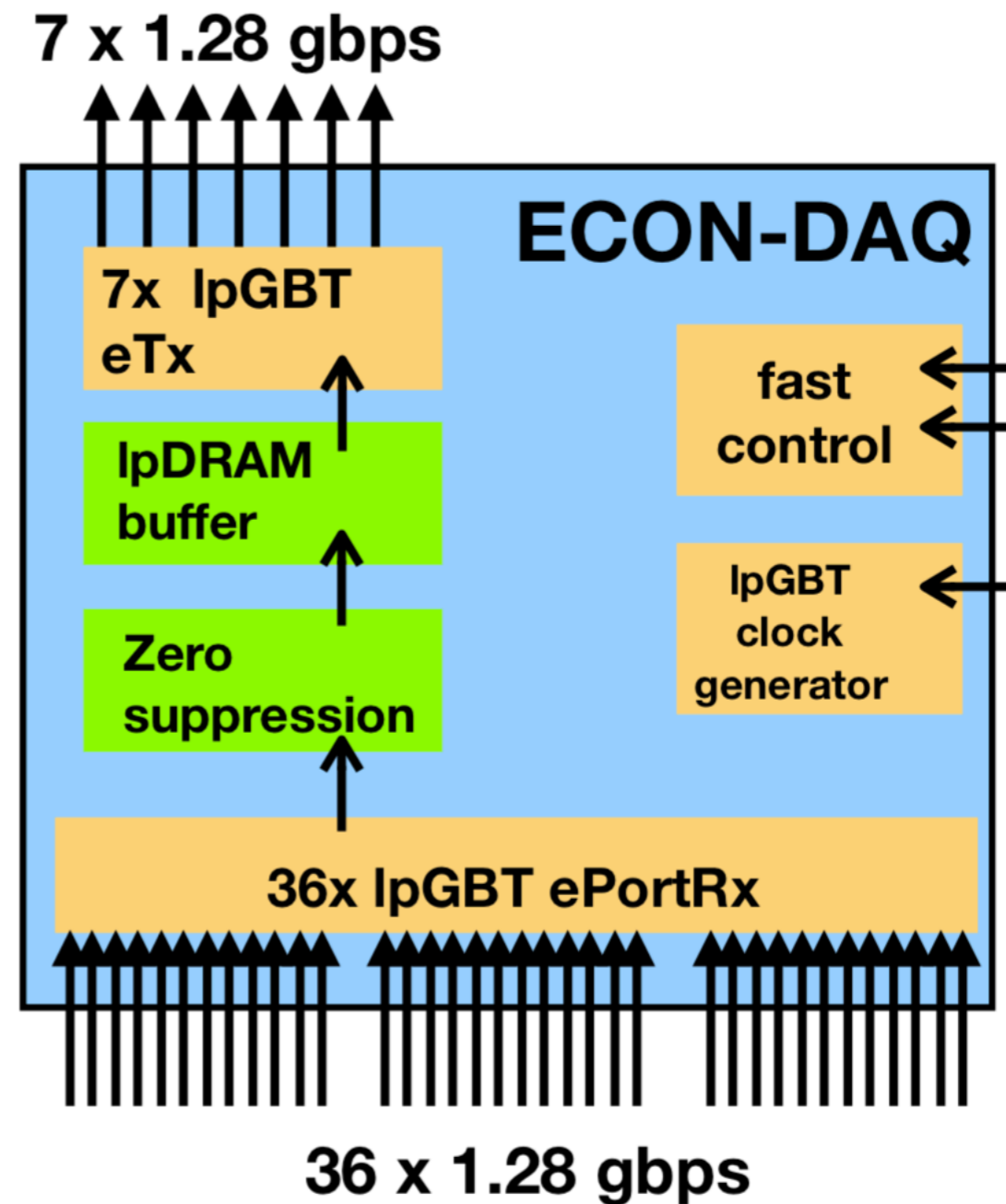
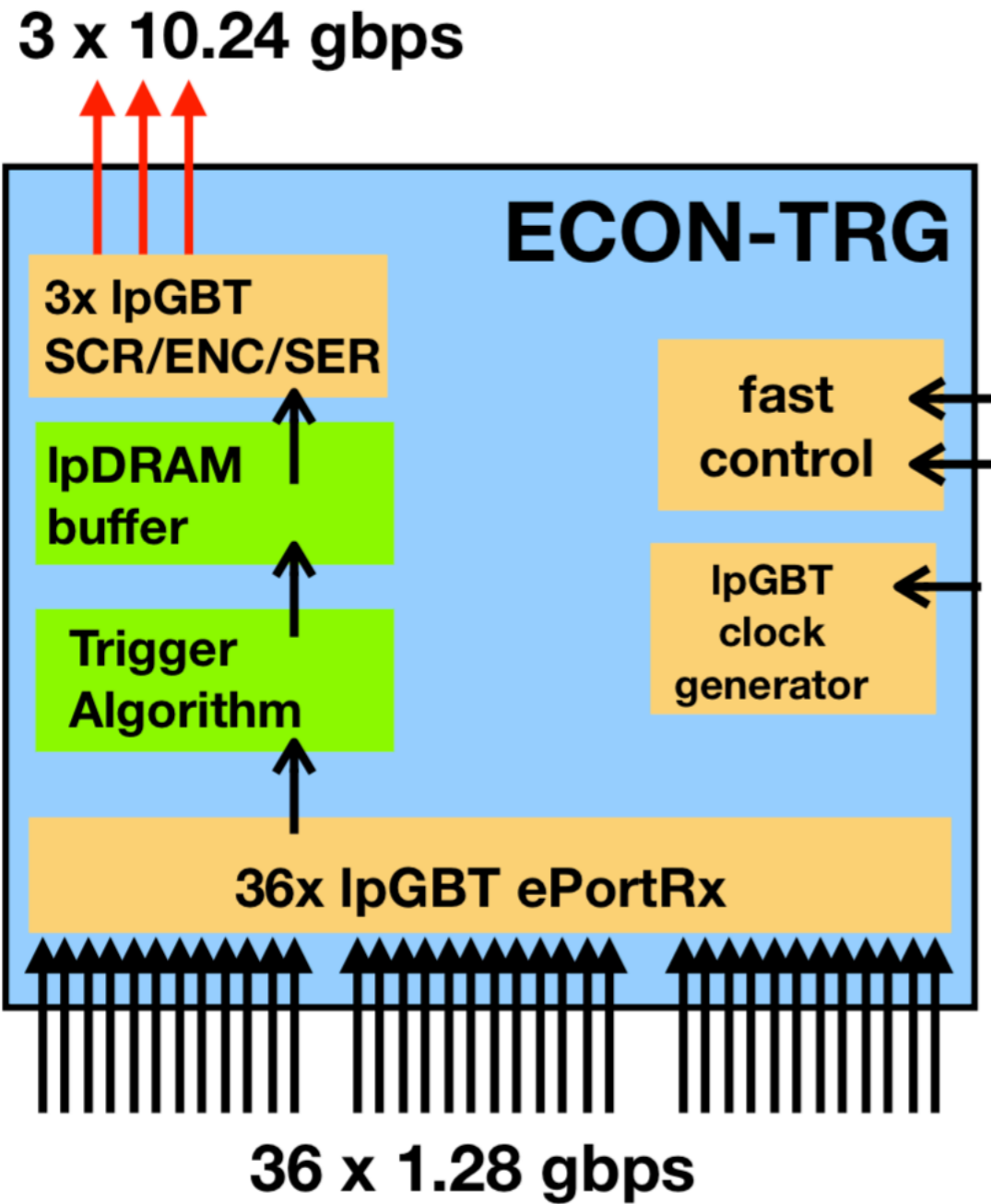


- Muon identification efficiency versus probability per event that another non-muon track identified as a muon
- Different noise scenarios explored consistent with last 12 layers of the HGAL

- Muon identification efficiency versus $|\eta|$ for $p_T > 5$ GeV



ECON





Test Beams since 2018



- H1: The DAQ System of the 12,000 Channel CMS High Granularity Calorimeter Prototype
- H2: Construction and Commissioning of CMS CE prototype silicon modules
- H3: Measurement of the response of a CMS HGCAL silicon-pad calorimeter prototype to electrons at the 2018 beam tests
- H4: First Tests of CMS HGCAL silicon using SKIROC2-CMS ASIC at the DESY II Beam Test
- H5: Timing performance of prototype silicon-sensor modules for the HGCAL in high-energy positron and pion beams at CERN
- C1: Hadron reconstruction performance of a CMS HGCAL+AHCAL prototype in beam tests

Jinst PUBLISHED BY IOP PUBLISHING FOR SISSA MEDIALAB

TECHNICAL REPORT

RECEIVED: December 3, 2020
ACCEPTED: February 1, 2021
PUBLISHED: April 20, 2021

Construction and commissioning of CMS CE prototype silicon modules

Jinst PUBLISHED BY IOP PUBLISHING FOR SISSA MEDIALAB

TECHNICAL REPORT

RECEIVED: December 2, 2020
ACCEPTED: February 2, 2021
PUBLISHED: April 15, 2021

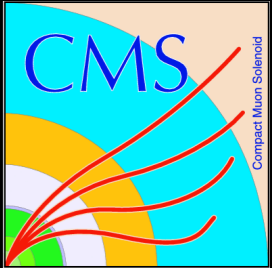
The DAQ system of the 12,000 channel CMS high granularity calorimeter prototype

B. Acar,^c G. Adamov,^b C. Adloff,^{ag} S. Afanasiev,^x N. Akchurin,^{ao} B. Akgün,^{c,e,*} M. Alhousseini,^w J. Alison,^f G. Altopp,^d M. Alyari,ⁱ S. An,^f S. Anagul,^g I. Andreev,^v M. Andrews,^f P. Aspell,^e I.A. Atakisi,^c O. Bach,^h A. Baden,^{ab} G. Bakas,^{ah} A. Bakshi,ⁱ S. Banerjee,ⁱ P. Bargassa,^z D. Barney,^e E. Becheva,^{aa} P. Behera,^r A. Belloni,^{ab} T. Bergauer,^l M. Besancon,^{al} S. Bhattacharya,^{ae} S. Bhattacharya,^{am} D. Bhowmik,^{am} P. Bloch,^s A. Bodek,^{ak} G. Bombardi,^e M. Bonanomi,^{aa} A. Bonnemaïson,^{aa} S. Bonomally,^s J. Borg,^s F. Bouyjou,^{al} D. Braga,ⁱ J. Brashear,^{ac} E. Brondolin,^e P. Bryant,^f J. Bueghly,^{ae} B. Bilki,^w B. Burkler,^d A. Butler-Nalín,^{ap} S. Callier,^{aj} D. Calvet,^{al} X. Cao,ⁿ B. Caraway,^a S. Caregarl,^{ag} L. Ceard,^{ai} Y.C. Cekmecelioglu,^c S. Cercl,^t G. Cerminara,^e N. Charitonidis,^e R. Chatterjee,^{ac} Y.M. Chen,^{ab} Z. Chen,^{ae} K.y. Cheng,^{ag} S. Chernichenko,^o H. Cheung,ⁱ C.H. Chien,^{ai} S. Choudhury,^p D. Čoko,^j G. Collura,^{ap} F. Couderc,^{al} L. Cristella,^e I. Dumanoglu,^g D. Dannheim,^e P. Dauncey,^s A. David,^e G. Davies,^s E. Day,^f P. DeBarbaro,^{ak} F. De Guio,^{ao} C. de La Taille,^{aj} M. De Silva,^h P. Debbins,^w E. Delagnes,^{al} J.M. Deltoro,^e G. Derylo,ⁱ P.G. Dias de Almeida,^e D. Diaz,^m P. Dinaucourt,^{aj} J. Dittmann,^a M. Dragicevic,^l S. Dugad,^{an} V. Dutta,^{ap} S. Dutta,^{am} J. Eckdahl,^{ap} T.K. Edberg,^{ab} M. El Berni,^{aj} S.C. Eno,^{ab} Yu. Ershov,^x P. Everaerts,^s S. Extier,^{aj} F. Fahim,ⁱ C. Fallon,^{ak} S. Fiorendi,^e B.A. Fontana Santos Alves,^e E. Frahm,^{ac} G. Franzoni,^e J. Freeman,ⁱ T. French,^e Y. Guler,^g E. Gurpinar Guler,^g

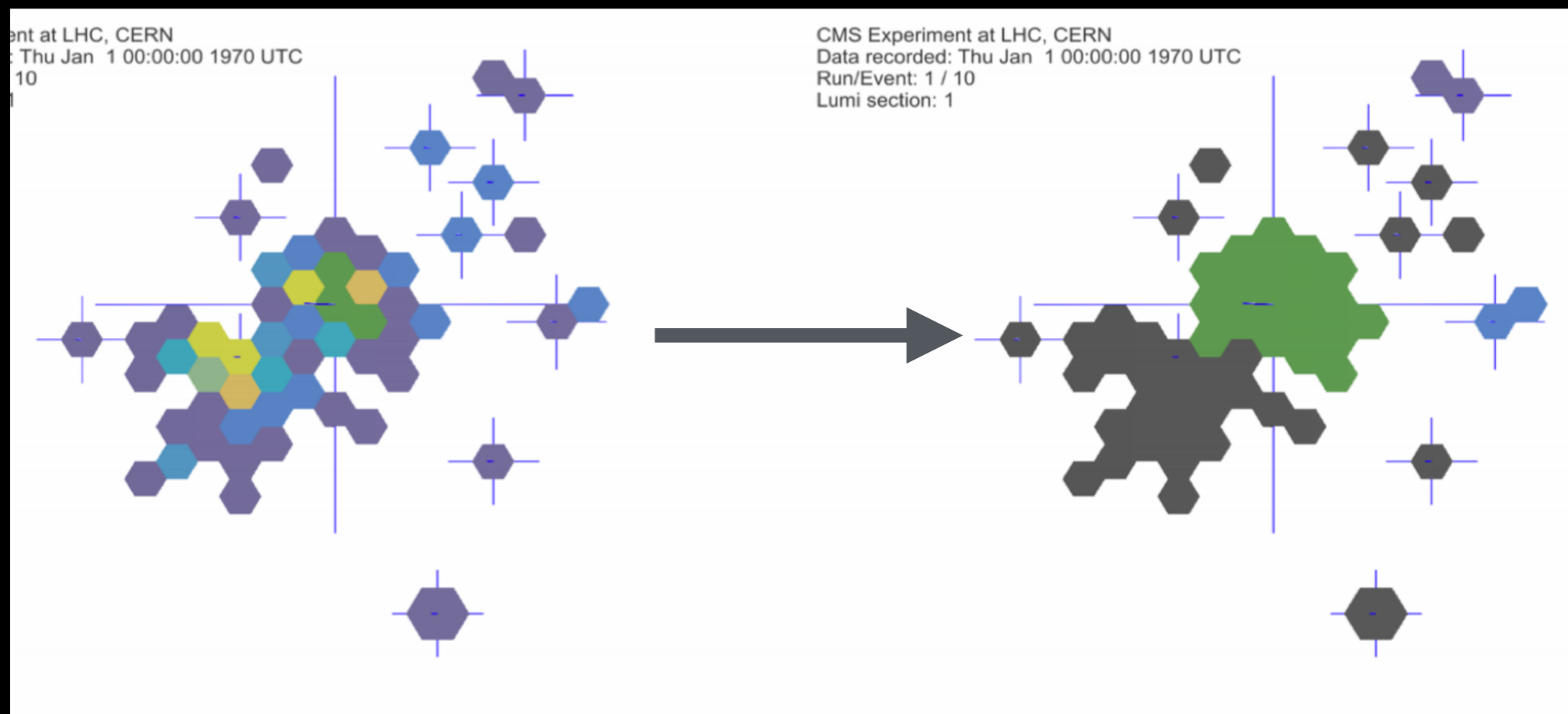
2021 JINST 16 T04



CLUE Algorithm

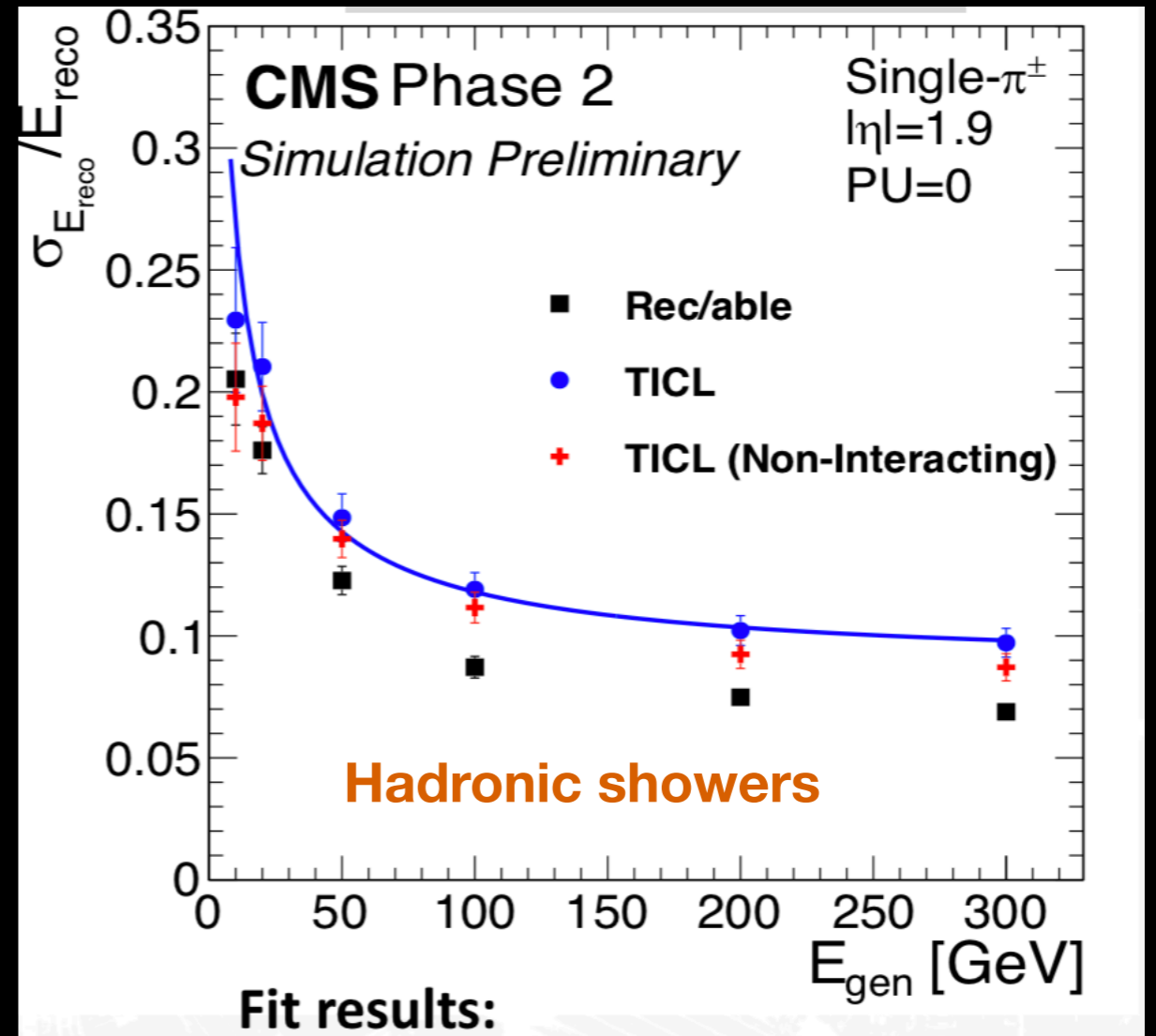
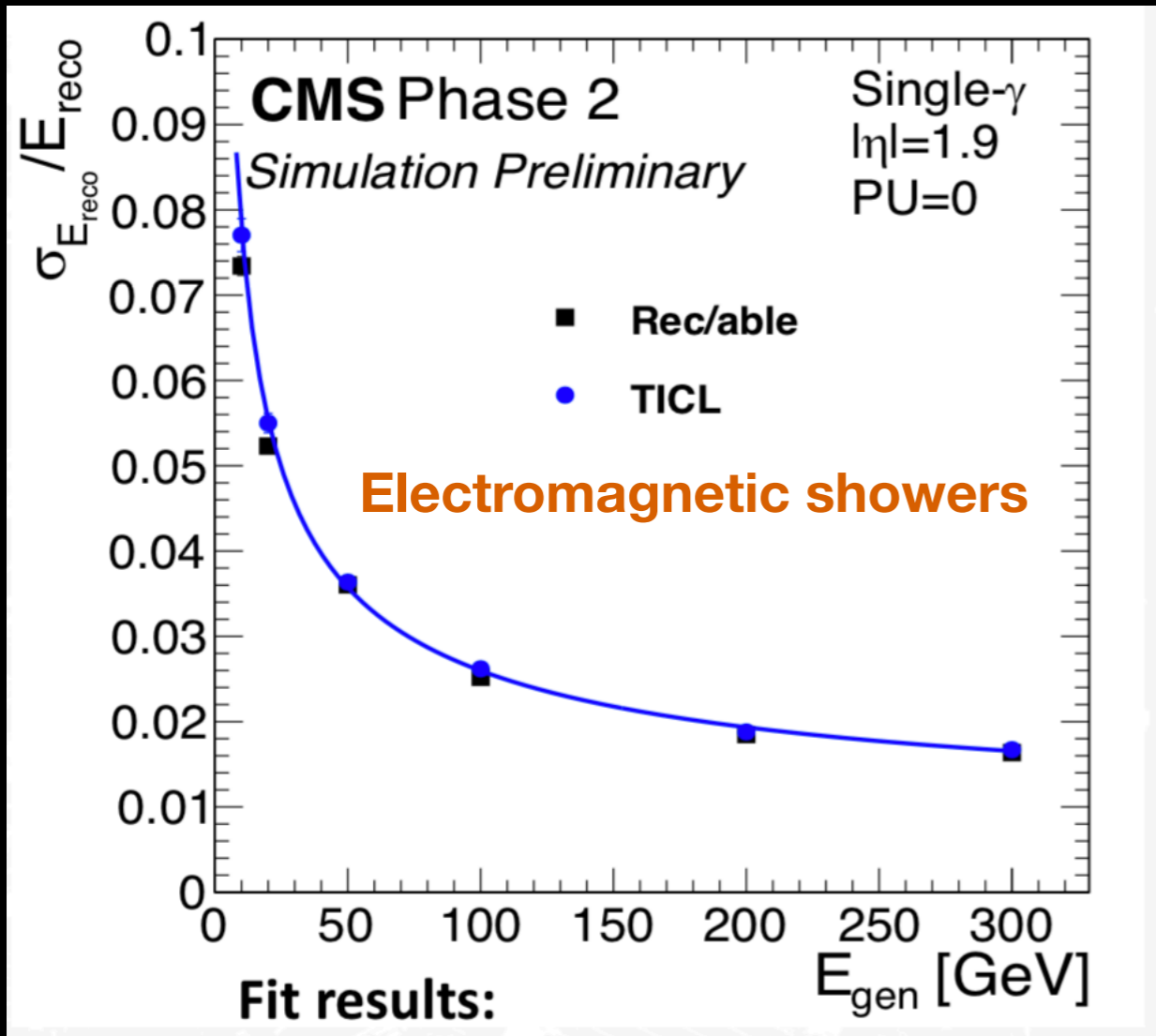
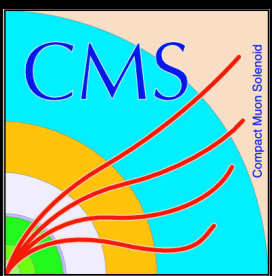


- Clustering: **CLU**stering by **E**nergy [CLUE] algorithm [arXiv:2001.09761]



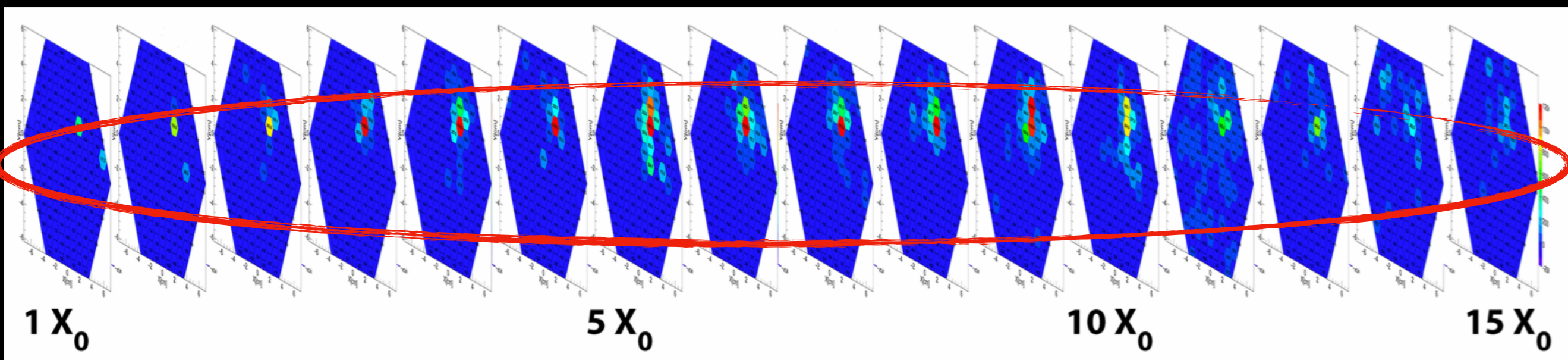


TICL Performance



	Stochastic	Constant
Rec/able	23%	0.9 %
TICL	25%	0.9 %

	Stochastic	Constant
Rec/able	72%	5.5 %
TICL	80%	8.7 %
TICL (Non-int/ing)	72%	8.0 %



- Simplified combinatorics if electromagnetic components removed before clustering hadronic block
- Linking of 2D layer clusters to form 3D shower performed with a cellular automaton based pattern recognition algorithm
 - Involves window search from layer $N \rightarrow$ layer $N+1$ including compatibility criteria based on energy, timing, geometric constraints

